Cerebral Cortex, December 2017;27: 5772–5783

doi: 10.1093/cercor/bhx254
Advance Access Publication Date: 28 September 2017
Original Article

ORIGINAL ARTICLE

Visual Cortex Limits Pop-Out in the Superior Colliculus of Awake Mice

Mehran Ahmadlou, Azadeh Tafreshiha and J. Alexander Heimel

Department of Cortical Structure and Function, The Netherlands Institute for Neuroscience, Royal Netherlands Academy of Arts and Sciences (KNAW), Meibergdreef 47, 1105 BA Amsterdam, The Netherlands

Address correspondence to J. Alexander Heimel. Email: heimel@nin.knaw.nl

Abstract

We detect objects more readily if they differ from their surroundings in motion, color, or texture. This increased saliency is thought to be related to increased responses in the visual cortex. The superior colliculus is another brain area involved in vision and especially in directing gaze and attention. In this study, we show that differences in texture orientation also increase responses in the superficial layers of the superior colliculus that receive retinal and cortical input. We found that gratings evoke more neural response when surrounded by orthogonal gratings than when surrounded by parallel gratings, particularly in the awake mouse. This pop-out is not originating from the visual cortex, and silencing visual cortex increased the relative difference in response. A model shows that this can result from retinotopically matched excitation from visual cortex to the superior colliculus. We suggest that the perceptual saliency of a stimulus differing from its surround in a low-level feature like grating orientation could depend on visual processing in the superior colliculus.

Key words: corticotectal connections, surround suppression, vision

Introduction

Visual features that differ from their surround catch our attention. The odd feature could signal a predator lurking in the bushes, or a prey trying to avoid capture. This perceptual pop-out also occurs if an oriented grating is presented on a background grating of another orientation (Joseph and Optican 1996; Parkhurst and Niebur 2004). In the primary visual cortex, the response to a grating surrounded by a similar orientation is smaller than when it is surrounded by a grating of an orthogonal orientation, in cats (Blakemore and Tobin 1972), monkeys (Knierim and van Essen 1992; Shushruth et al. 2013), humans (Vanegas et al. 2015), and rodents (Girman et al. 1999; Self et al. 2014). This cortical response pop-out effect is often assumed to be the source for the perceptual pop-out (Parkhurst and Niebur 2004; Boehler et al. 2009; Melloni et al. 2012; Zhang et al. 2012; Shushruth et al. 2013; Schmid and Victor 2014). The superior colliculus, however, is another brain structure involved in processing of visual information and is strongly involved in directing attention (Knudsen 2007; Zénon and Krauzlis 2012). Indeed, recently, neural pop-out effects have been found in the homologous optic tectum of archer fish and barn owls which both lack cerebral cortex (Zahar et al. 2012; Ben-Tov et al. 2015). The perceptual pop-out in mammals could thus also depend on visual processing in the superior colliculus if the response pop-out would be present there.

Neurons in the visually driven superficial layers of the superior colliculus (sSC) in rodents, like in primates, often have an optimal stimulus size, and stimuli larger than this size evoke smaller responses (Binns and Salt 1997; Girman and Lund 2007; Wang et al. 2010; Gale and Murphy 2014; Kasai and Isa 2016). The reduction of response to a center grating can depend on the orientation of the surround grating in a way similar to the response pop-out seen in cortex (Girman and Lund 2007). It is clear that both retinal input and local GABAergic inhibition

(Binns and Salt 1997; Kaneda and Isa 2013) contribute to surround suppression in the sSC, but it is unclear where this orientation dependence originates. Surround modulation in the sSC could also partially result from processing in the visual cortex. More than the superior colliculus, the visual cortex is thought to be involved in complex image analysis and it projects to the sSC. Any pop-out effect could be computed in visual cortex and imposed on the sSC through projections from V1 or higher visual areas (Itti and Koch 2001). The effect of V1 inactivation on the basic response properties in the sSC in the anesthetized animal is weak (Wang et al. 2010; Ahmadlou and Heimel 2015), but in the awake animal silencing V1 decreases the response gain to looming stimuli in the sSC (Zhao et al. 2014). The effect of corticotectal input on responses to center-surround grating stimuli in the awake sSC is unknown.

In this study, we used laminar extracellular recordings in the mouse sSC to characterize responses to gratings in the presence and absence of stimulus surrounds and the influence of visual cortex on this modulation. We find that under anesthesia iso-oriented surround suppression is stronger in the upper sSC than in the lower sSC. There is much less reduction for surrounding gratings with an orthogonal orientation, especially in the awake animal. The relative response difference is larger in the sSC than in V1 and cortical silencing in awake mice increases the relative strength of response in the sSC to an orthogonal surround compared to that of a parallel surround. We model the input of cortex to the sSC by retinotopically matched excitatory connections and this captures the influence of visual cortex on the orientation specificity of the surround suppression. The cortical input will influence which stimuli lead to a behavioral response through the collicular pathway. Its function can be interpreted as a reduction of the animal's reliance on low-level image features to compute saliency.

Materials and Methods

C57BL/6JOlaHsd (Harlan) mice of 1.5–4 months old were used for the experiments. Mice were housed in a 12/12 h dark/light cycle and experiments were carried out during the light phase. All experiments were approved by the institutional animal care and use committee of the Royal Netherlands Academy of Arts and Sciences.

Surgery for Anesthetized Recording

Mice were anesthetized by an intraperitoneal injection of 1.2 g urethane per kg body weight, supplemented by a subcutaneous injection of 8 mg chlorprothixene per kg body weight. We injected atropine sulfate (0.1 mg per kg) and dexamethasone (4 mg per kg) subcutaneously to reduce mucous secretions and to prevent cortical edema, respectively. Additional doses of urethane were injected when a toe-pinch response was observed. Mice were head fixed by ear and bite bars. Small craniotomies for recording were made by dental drill. Temperature was measured with a rectal probe and maintained by a feedback-controlled heating pad set to 36.5 °C. Animals were euthanised at the end of the recording session by an overdose of urethane and spinal dislocation, or, when used for perfusion, by an overdose of pentobarbital (100 mg/kg i.p.).

Surgery for Awake Recording

For awake recordings, mice were first anesthetized with isoflurane (5% induction, 1.2–1.5% maintenance) in oxygen (0.8 l/min flow rate). Rectal temperature was maintained at 36.5 °C. The eyes were protected from light by black stickers and from drying by Cavasan eye ointment. During their surgery, mice were administered the analgesic Metacam (1 mg/kg s.c.) to reduce pain during the recovery. Mice were head fixed and the scalp and soft tissue overlying the skull were incised to expose the skull. A metal ring (5 mm inner diameter) was attached to the skull with glue and dental cement. Small craniotomies for recording were made by dental drill. Next, the head was fixed to a stand through a handle attached to the ring. Animals recovered for 2 h before the recordings started. The animals were given water and milk in the first hour after recovery, while they were restrained. Animals were euthanised at the end of the recording session by an overdose of pentobarbital (100 mg/kg i.p.).

Electrophysiological Recording

Laminar silicon electrodes (A1 × 16-5 mm-50–177, 16 channels spaced 50 μm apart, Neuronexus) were used for extracellular recordings. For recordings in the superior colliculus, electrodes were inserted vertically through a craniotomy 500–1000 μm lateral and 300–900 μm anterior to the Lambda cranial landmark. The literature (Cang et al. 2008; Wang et al. 2010; Ahmadlou and Heimel 2015) and our measurements of receptive field positions showed that this is the binocular region of the sSC. The surface of the sSC was determined by the first visual response. There was considerably less visual responsiveness 350–400 μm after the first visual response, matching the thickness of the sSC described in the literature (Wang et al. 2010; Ahmadlou and Heimel 2015) and the mouse brain atlas (Allen Brain Institute; http://mouse.brain-map.org/static/atlas). This meant that 7 or 8 channels of the laminar probe were in the sSC. In the case of 7 channels, we labeled the top 2 as uSGS, the middle 3 as lSGS and the bottom 2 as SO. For 8 channels, these numbers were 3, 2, 3. The CSD analysis confirmed the channels of SO, as it showed a sink consistent with the strong retinal input (Zhao et al. 2014). For the experiments on the influence of visual cortex on the sSC, we used a second laminar silicon electrode (the same type as used in the sSC) and simultaneously recorded from the binocular region of V1 (2900–3000 μm lateral and 300–500 μm anterior to Lambda). The signals were digitized at 24 kHz and bandpass filtered between 500 Hz–10 kHz using a Tucker-Davis Technologies RX5 pentusa. Signals were thresholded at 5x standard deviation to isolate spikes, and spikes were sorted into single-units by custom-written Matlab (Mathworks) scripts using the first set of principal components of the spike wave forms and k-means based clustering. Resulting clusters and wave forms were checked visually for the goodness of isolation. For most of the analysis in the manuscript, however, single and multi-units were pooled together to increase the number of measurements, unless otherwise stated. Minimum evoked visual response for a unit to be included was 1.5 Hz.

Histology

When needed to ascertain the location of a DiI-coated electrode, or to measure the extent of the fluorescent muscimol diffusion, we transcardially perfused the mice with 4% paraformaldehyde (PFA) in phosphate buffered saline (PBS), and post-fixated the brains for 2 hours in PFA at 4 °C before moving the brain to a PBS solution. Later, we cut the brains in coronal slices of 50 μm thickness on a vibratome. We mounted the sections using Vectashield mounting medium containing DAPI. The slides were imaged on an Axioplan 2 Zeiss fluorescence microscope using a 5x objective

with 546 nm excitation light to visualize DiI and fluorescent muscimol and 365 nm light for DAPI.

Visual Stimulation for Electrophysiology

Stimuli were projected by a gamma-corrected PLUS U2-X1130 DLP projector onto a back projection screen (Macada Innovision, covering a 75 × 57 cm area), positioned 17.5 cm in front of the mouse. Gamma-correction was done using a Minolta LS-100 luminance meter and custom Matlab scripts using the PsychToolbox gamma-fitting routines. Background luminance was 100 cd/m^2 at the center of the screen in the direction of the mouse. To determine receptive field location, we presented a 5 min movie (5 frames per second) of small white squares (5 deg) in random positions on a black background (ratio of white to black area: 1/30, Heimel et al. 2010). The visual stimuli were produced using Psychophysics Toolbox 3 (Kleiner et al. 2007). To measure size tuning and the surround suppression index, we showed circular patches of drifting, square wave, gratings, centered at the receptive field location. The diameters of the patches were 15, 25, 40, 60, 90, and 120 deg when presented directly in front of the animal. The same physical sizes were also used on the other positions centered on the receptive field of the recording site. For computing the optimal diameter, we later computed the real visual angle based on the stimulus location relative to the mouse. Outside the stimulus patch the monitor remained an equiluminant grey. The gratings were drifting in 8 or 16 different directions (with steps of 22.5–45 deg) with 0.05 cpd (in front of the mouse) at 95% contrast. The same physical grating spacing was used for the entire screen. No correction was made to adjust for the distance on the projection screen to the mouse. For the range of receptive field centers that we encountered in this study, the maximal apparent spatial frequency would be 0.07 cpd (for the calculation, see Ahmadlou and Heimel 2015). Drift speed was 2 Hz. The stimuli used for measuring cross-orientation facilitation consisted of the same drifting gratings in a circular patch with a diameter that was the preferred size plus 10 deg (called center), surrounded by an annulus with a grating drifting in the same direction as the center grating (called iso-oriented surround) or drifting at an orthogonal direction (called cross-oriented surround). The outer diameter of the annulus was 110 degrees. We also showed the surrounding annulus (parallel to the iso-oriented surround) without a center grating. These 4 different stimuli were shown for all 16 or 8 directions of the center stimulus. The stimulus and interstimulus duration were both 1 s. The stimuli were presented pseudorandomly, and at least 5 repetitions of each unique stimulus were used to compute responses.

Silencing Visual Cortex

For measuring the influence of the visual cortex on the sSC, where we required broad reduction of activity in the visual cortex, we injected 100–150 nl of 2 mM fluorescent muscimol (BODIPY TMR-X conjugate, Life Technologies), an agonist of $GABA_A$ receptors, in binocular V1 at 2 depths (300 and 500 μm below dura) using a Drummond Nanoject2 volume injector (with volume rate of 2.3 nl per second). This was done while laminar probes were present in the binocular sSC and V1. The recording location in V1 was the same location (within 0.1 mm) in which muscimol was injected. The histology showed this amount of muscimol was enough to cover most of V1.

Pupil Tracking

A headpost was attached under isoflurane surgery, similar to the method described in the section on surgery for awake recording. After full recovery, the awake animal was head fixed in the electrophysiology setup. The mouse was presented with a series of stimuli (center grating, center plus iso-oriented surround, center plus cross-oriented surround, annulus) with sizes and stimulus center locations similar to those used for the electrophysiological recordings. One eye was illuminated with an IR-led and continuously video recorded with a Basler acA640-90um infrared-sensitive monochrome CCD camera throughout the session. The pupil position and dilation were automatically determined from the video by a custom-written C-program (available at github.com/heimel/InVivoTools/Physiology).

Pupil position and radius were measured in camera pixels and converted to estimated mouse viewing angles. The estimate was done by making the approximations that the eye is spherical and that an eye movement is a rotation around the center of the eye, and by estimating the radius of the eye from the image, aided by previous experience with enucleation. The x and y axis are arbitrary and do not correspond with horizontal and vertical view directions. For the analysis, we computed the displacement as the absolute difference in viewing angles (in degrees) from the median pupil position over the entire session. This is invariant under a rotation in x and y. For each stimulus, the change in displacement or radius was calculated as the mean displacement or radius over the entire 1 s duration of a stimulus minus the mean displacement or radius in the last 0.25 s before stimulus onset. Per test session, we computed the mean change in radius and displacement of each stimulus type (center, center+iso-surround, center+cross-surround and annulus) over all directions.

To compare the distribution of pupil positions and speeds across animals, we rotated the camera x-y plane from the image to the horizontal and vertical viewing directions of the animals. We did this by rotating the x-y distribution, which was always clearly elongated in one direction, such that the longest distribution-axis became the horizontal axis. We computed the distribution of pupil positions in the horizontal-vertical plane during the stimulus presentation, relatively to the position in the last 0.25 s before stimulus onset. These distributions we compared for the different stimulus types, at different timepoints after stimulus onset. Using the horizontal and vertical pupil positions, we computed for each imaged frame the horizontal and vertical speeds as the difference in position compared to the previous frame in degrees per second. We compared the distribution of speeds at different timepoints after stimulus onset.

Data Analysis

Analysis was done using Matlab scripts available online at https://github.com/heimel/InVivoTools, a fork from code written by Steve Van Hooser. Current source density (CSD) analysis was used for the laminar probe records to illustrate the current flow at different depths of the sSC. The local field potentials (LFPs) of i'th channel in response to visual stimuli were averaged across all trials, and indicated by L_i. Then the CSD profile was derived by computing the second spatial derivative across the channels. The CSD of the i'th channel is $(2\,L_i - L_{i-1} - L_{i+1})/\Delta^2$, where Δ is the distance between 2 neighboring channels. For all the analysis of spiking activity, the responses were averaged over all directions of the center grating, but the results were not qualitatively

different when the optimal direction or orientation was used. The rate was the average firing rate during the entire interval that the stimulus lasted (1 s). Whenever we use the word response, we refer to the rate minus the spontaneous rate. The spontaneous rate was defined as the mean rate in the 0.5 s before stimulus onset. The surround suppression index (SSI) was defined as $(R_{pref} - R_{largest})/R_{pref}$, where R_{pref} is maximum response and $R_{largest}$ is the response to the largest stimulus. The orientation-specific suppression index (OSSI) was calculated as $(R_{cross} - R_{iso})/(R_{cross} + R_{iso})$, where R_{cross} is the mean response to the stimulus of center with a cross-oriented surround, and R_{iso} that of a stimulus with an iso-oriented surround. Analogous to the SSI (but opposite in sign), we defined a cross-orientation facilitation index (COFI) as $(R_{cross} - R_{pref})/R_{pref}$. The SSI and OSSI are not normally distributed, because responses are mostly positive and these indices are thus soft-limited between 0 and 1 (SSI) and –1 and 1 (OSSI). For this reason, all statistical tests involving these indices are non-parametric Mann–Whitney *U*-test when 2 independent groups were compared, or Kruskal–Wallis when 3 or more groups were compared. For comparison of laminar differences, we first used a Kruskal–Wallis test, followed by Bonferroni corrected tests for all layers versus each other. When the same units were compared in 2 conditions, the paired non-parametric signed rank test was used. For the visual presentation of medians, we computed the bootstrapped standard error in the medians. This was done by recomputing the median n times by resampling with reuse from the original samples and computing the standard deviation of the result, where n is the smallest integer larger than 100,000/sample size.

Model

The model is a phenomenological description of a population of rate-based sSC neurons, which get excitatory input from the retina and other sSC neurons, inhibitory input from other sSC neurons, and excitatory input from the visual cortex.

The response in the stationary state of neuron i to visual stimulus stim is given by

$$R(\mathrm{i}, \mathrm{stim}) = E(\mathrm{i}, \mathrm{stim}) - I(\mathrm{i}, \mathrm{stim}) + F(\mathrm{i}, \mathrm{stim}),$$

where E(i, stim) is the stimulus-dependent excitatory input, I(i, stim) the inhibitory input, and the response fluctuation term F(i, stim) is a normal random variable with mean 0 and standard deviation σ. The visual stimulus stim could be either center, iso or cross, where we take center to mean a central patch of drifting grating, iso the same center patch with an iso-oriented surround and cross the center patch with a cross-oriented surround. The receptive field of the model neurons is not explicitly modeled, but we assume that it matches the extent of the center stimulus.

The excitation has 2 components, $E(\mathrm{i}, \mathrm{stim}) = E_{rs}(\mathrm{i}, \mathrm{stim}) + E_{ctx}(\mathrm{stim})$, where E_{rs} is excitatory retinal and local input and E_{ctx} is the corticotectal input. The excitatory retinal and local input E_{rs} of neuron i to the center stimulus in its receptive field is an exponentially distributed random variable D:

$$E_{rs}(\mathrm{i}, \mathrm{center}) = D(\mathrm{i})$$

The excitatory retinal and local input to the iso and cross stimuli are:

$$E_{rs}(\mathrm{i}, \mathrm{iso}) = E_{rs}(\mathrm{i}, \mathrm{center})(1 - \mathrm{SSI}_{rs})N(\mathrm{i}, \mathrm{iso})$$
$$E_{rs}(\mathrm{i}, \mathrm{cross}) = E_{rs}(\mathrm{i}, \mathrm{center})(1 - \mathrm{SSI}_{rs})(1 + \mathrm{OSSI}_{rs})/(1 - \mathrm{OSSI}_{rs})N(\mathrm{i}, \mathrm{cross})$$

where N(i, iso) and N(i, cross) are normally distributed random variables with mean 1 and standard deviation V. By choosing the input like this, we ensure that

$$\mathrm{SSI}_{rs} = (ME_{rs}(\mathrm{center}) - ME_{rs}(\mathrm{iso}))/ME_{rs}(\mathrm{center})$$
$$\mathrm{OSSI}_{rs} = (ME_{rs}(\mathrm{cross}) - ME_{rs}(\mathrm{iso}))/(ME_{rs}(\mathrm{cross}) + ME_{rs}(\mathrm{iso})),$$

where $ME_{rs}(\mathrm{stim}) = 1/N \sum_i E_{rs}(\mathrm{i}, \mathrm{stim})$ and N is the number of cells in the sSC.

Cortical input is retinotopically matched and is given by

$$E_{ctx}(\mathrm{center}) = \varepsilon_{ctx} ME_{rs}$$
$$E_{ctx}(\mathrm{iso}) = E_{ctx}(\mathrm{center})(1 - \mathrm{SSI}_{ctx})$$
$$E_{ctx}(\mathrm{cross}) = E_{ctx}(\mathrm{iso})(1 + \mathrm{OSSI}_{rs})/(1 - \mathrm{OSSI}_{rs}),$$

such that the SSI and OSSI of the cortical excitation in the model matches the SSI and OSSI that we measured in V1.

The local inhibition I_{sc} in the model is purely a surround inhibition. It is absent for the center stimulus and is activated by stimuli in the surround of the center stimulus. It can thus be thought of as activated by the responses of neurons with receptive fields that are neighboring the modeled population. The inhibition scales in proportion to the activation of the modeled neurons, using the assumption that the neuronal populations with receptive fields covering the surrounds of the iso and cross stimuli are activated in the same manner as the model neurons:

$$I_{sc}(\mathrm{i}, \mathrm{center}) = 0$$
$$I_{sc}(\mathrm{i}, \mathrm{iso}) = \iota_{sc} E(\mathrm{i}, \mathrm{iso})$$
$$I_{sc}(\mathrm{i}, \mathrm{cross}) = \iota_{sc} E(\mathrm{i}, \mathrm{cross})$$

Finally, cells with a maximum response for all stimuli below 1.5 Hz are removed from the sample to comply with our treatment of the recorded cells. This does not influence the model results.

In the model the SSI and OSSI of V1 are taken as given. The free parameters of the model are the SSI and OSSI of the retinal and local excitatory input (SSI_{rs}, OSSI_{rs}), the relative strength of local inhibition ι_{sc}, the strength of cortical input ε_{ctx}, the distribution width of excitatory input strength D, the variability in the mean response properties of individual neurons V, and the response variability σ. The values for the free parameters in the model used for the figure in the manuscript are $\mathrm{SSI}_{rs} = 0.4$, $\mathrm{OSSI}_{rs} = 0.51$, $\iota_{sc} = 0.38$, $\varepsilon_{ctx} = 0.28$, $D = 9$, $V = 0.3$, $\sigma = 0.15$. These values could not be derived from the literature but were chosen to reproduce the measurements and found by minimization (using Matlab fminsearch and a loop over different initial conditions) of the sum squared difference of the mean and standard deviations of SSI, OSSI and responses for the iso-oriented surround in the superior colliculus with and without visual cortex in the model and the measurements (Table 1). To compute the values in Table 1 and the probability distribution in Figure 4, the model was computed with 1 000,000 cells, but the results are independent of the number of cells if it is sufficiently large.

Results

Laminar Profile of Surround Suppression in the sSC

First, we wanted to characterize the surround modulation across the superficial layers of the superior colliculus. We performed extracellular recordings with linear silicon probes spanning the entire sSC in head fixed anesthetized mice and mice that had awoken from anesthesia (Fig. 1*A*). Current source density plots (Fig. 1*B*) show an early sink which indicates the stratum opticum (SO), the sublayer of the sSC where the retinal axons enter (Zhao et al. 2014). The layer above the SO is the stratum griseum superficiale (SGS). The visual evoked activity

Table 1. Match of model observables to experimental averages. Model results are averages over 1 000,000 cells. Experimental data are mean ± SEM.

			Silenced visual cortex	
	Model	Experimental data	Model	Experimental data
Response to grating with iso-oriented surround	3.7 Hz	3.8 ± 0.6 Hz	2.9 Hz	2.9 ± 0.5 Hz
SSI	0.62	0.62 ± 0.03	0.62	0.62 ± 0.04
OSSI	0.41	0.42 ± 0.02	0.49	0.48 ± 0.03

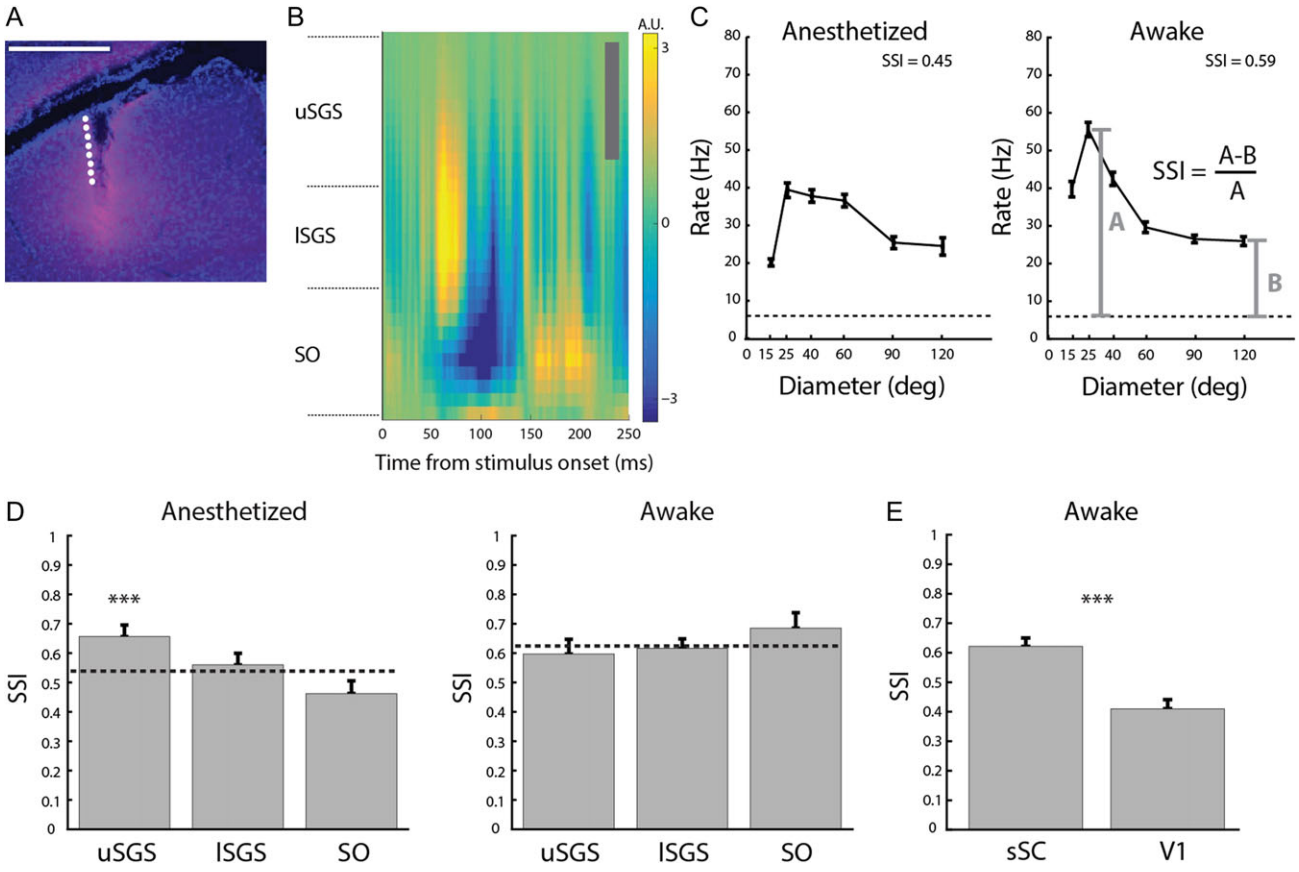

Figure 1. The laminar profile of surround suppression in the sSC. (*A*) Example of a laminar probe track, visible with red DiI in the sSC. Blue is DAPI. Scale bar indicates 0.5 mm. White dots give an impression of the channel spacing of the recording laminar probe (distance between sequential channels is 50 μm). (*B*) Example of current source density plot in sSC showing an initial current sink in the SO (blue) and a source in the upper layer of the sSC. Scale bar is 100 μm. (*C*) Examples of size tuning in the sSC in anesthetized and awake mice. Dashed lines show level of spontaneous firing. Error bars show mean over 16 directions and intertrial SEM (5 repetitions per direction). (*D*) Laminar profile of surround suppression index (SSI) in the sSC of anesthetized (left) and awake (right) mice. Error bars show population median and bootstrapped error. Dashed lines show the mean SSI over the entire sSC. ***Denotes $P < 0.001$ for both comparisons to other layers. (*E*) SSI in the sSC and V1 of awake mice. Error bars show population median and bootstrapped error. ***Denotes $P < 0.001$.

in the anesthetized animal usually extended over about 300 μm. Recordings in the lowest (ventral) 100 μm with visual activity we assigned to the SO. The top 100 μm was very likely in the SGS and we assigned to the upper SGS (uSGS). The middle 100 μm could not be assigned with certainty to either the SO or SGS, and we labeled recording contacts at these depths as lower SGS (lSGS). We started by mapping the receptive field center for the single and multi-units on all the recording sites by showing a sparse random distribution of white squares on a black background. The patch evoking the maximum ON or OFF response was considered the receptive field center. Usually the RFs were centered at the same spatial location for all recording sites of a probe that were within the sSC, but when this was not the case we either selected one and ignored the other sites for the subsequent analysis, or showed the stimuli multiple times centered at the different RF centers. Next, we showed circular patches of a range of diameters with drifting gratings, centered at the receptive field center. Many neurons in mouse sSC respond well to gratings and show orientation selectivity (Wang et al. 2010; Feinberg and Meister 2015; Ahmadlou and Heimel 2015). Across the sSC, we often found strong reduction of responses for larger stimulus sizes, both in the awake and anesthetized animal (Fig. 1*CD*). We found that under anesthesia the strength of surround suppression, as quantified by the surround suppression index (SSI, Fig. 1*C*), was different in the different layers of the sSC ($P = 0.00004$, Kruskal–Wallis test, uSGS:86, lSGS:85, SO:86

units, 14 mice, Fig. 1D), with more surround suppression in the uSGS than in the SO and lSGS. This laminar profile disappeared when the animal was awake ($P = 0.18$, Kruskal–Wallis test, uSGS:58, lSGS:49, SO:58 units, 12 mice, Fig. 1D). Median optimal grating diameter was lower in the uSGS than in the SO both under anesthesia and in the awake animal (Supplementary Fig. 1). Over all layers together, the amount of surround suppression in the awake animal was higher than in the anesthetized condition (anesthetized: SSI = 0.58 ± 0.02, awake: SSI = 0.62 ± 0.02, median ± bootstrapped error, $P = 0.01$, Mann–Whitney U-test). This higher SSI in the awake was due to an increase in suppression and not due to an increased center response, which was slightly lower in the awake animal (anesthetized: 17.7 ± 2.6 Hz, median ± bootstrapped error, awake: 12.2 ± 1.5 Hz, $P = 0.02$, Mann–Whitney U-test). The spontaneous rate was slightly increased in wakefulness (anesthetized: 1.0 ± 0.2 Hz, awake: 1.6 ± 0.4 Hz median ± bootstrapped error, $P = 0.004$, Mann–Whitney U-test). To compare, we also recorded in V1. In accordance with previous studies in awake mice, we found surround suppression in V1 (Adesnik et al. 2012; Vaiceliunaite et al. 2013; Pecka et al. 2014), but it was weaker than in the sSC (sSC: SSI = 0.62 ± 0.02, V1: SSI = 0.40 ± 0.04, median ± bootstrapped error, $P < 0.000001$, Mann–Whitney U-test, 34 cortical units, 5 mice, Fig. 1E).

Pop-Out of Cross-Oriented Gratings

Once we had determined the size tuning profiles, we selected the diameter that was optimal for most of the recording sites that shared a receptive field center on the penetration. Next, we showed gratings of this optimal diameter plus 10 degrees, surrounded by background gray, or an iso-oriented (parallel) or cross-oriented (orthogonal) grating annulus with a 110 degree outer diameter (Fig. 2A). In addition, we showed an annulus grating without any center grating. The surrounding annulus by itself generally caused little response. Most cells showed a strong reduction when the center grating was surrounded by an iso-oriented grating as indicated before, but only very little reduction or even an increase if surrounded by an orthogonal grating (Fig. 2B,C). The response to stimuli of a center with an orthogonal surround was slightly larger than the response to center alone (difference 0.57 ± 0.20 Hz, mean ± SEM, $P = 0.0006$, Wilcoxon signed rank test). The difference in rates between the parallel and orthogonal surround develops at the same time as the surround suppression and starts from the beginning of the stimulus response (Fig. 2B inset). We quantified the pop-out effect of a center grating with a cross-oriented surround compared to an iso-oriented surround with an orientation-specific suppression index (OSSI, Fig. 2A). In the awake mouse the difference in response between gratings with a cross-oriented surround and an iso-oriented surround was even more pronounced than under anesthesia ($P < 0.001$, Mann–Whitney U-test, Fig. 2D). This difference in responses was not due to the presence of eye movements in the awake animals, because for each stimulus condition average pupil position per trial did not deviate further from the median pupil position than just before stimulus onset (Supplementary Fig. 2–4 and Supplementary Movie). The mean displacement and the speed did not change after onset of any of the visual stimuli ($P > 0.05$ for all stimuli, Supplementary Fig. 2 F-G). In addition, the distributions of pupil positions and pupil velocity were not different for the different stimulus conditions after stimulus onset (Supplementary Fig. 3–4). Compared to the other layers, the OSSI was lower in the uSGS in the awake ($P = 0.0027$, Kruskal–Wallis, uSGS:33, lSGS:39, SO:33 units, 13 mice, Fig. 2D) but there was no difference between the layers in the anesthetized condition ($P = 0.95$, Kruskal–Wallis, uSGS:25, lSGS:23, SO:25 units, 6 mice, Fig. 2D).

We also showed the same stimuli in the primary visual cortex of awake mice. Although the difference between a cross- and an iso-oriented surround is present there, as was also previously reported (Self et al. 2014), the relative difference is much higher in the sSC (OSSI sSC: 0.45 ± 0.02, V1: 0.22 ± 0.05, median ± bootstrapped error, $P < 0.001$, Mann–Whitney U-test, Fig. 2E). This is unlikely to be due to a different pooling of single-unit responses into multi-units, because for isolated single-units in the sSC we do not find a lower SSI (single-units: 0.71 ± 0.05, median ± bootstrapped error, $P = 0.96$, Mann–Whitney U-test, 20 single units) and the OSSI is even higher for single than for multi-units (single-units: 0.62 ± 0.05, median ± bootstrapped error, $P = 0.03$, Mann–Whitney U-test, Supplementary Fig. 5). The differences in absolute rates between cross- and iso-oriented surrounds appear in V1 and sSC at about the same time (Fig. 2E inset).

Cortical Input Decreases Pop-Out of Cross-Oriented Stimulus

Previously, we and others have shown that there is little influence of the visual cortex on responses in the sSC in the anesthetized mouse (Wang et al. 2010; Ahmadlou and Heimel 2015). Under anesthesia, cortical ablation did not change contextual modulation in the rat uSGS (Girman and Lund 2007). In the awake mouse, however, silencing of visual cortex reduced the gain of sSC responses to looming stimuli, without changing the speed tuning (Zhao et al. 2014), and surround suppression can be dependent on the state of the animal, at least in V1 (Ayaz et al. 2013). Therefore, we wanted to understand the influence of the corticotectal projection on more complicated stimuli in the awake animal. We measured surround modulation in the sSC and V1 in awake mice, and subsequently silenced the visual cortex by injecting the $GABA_A$ receptor agonist muscimol (fluorescently conjugated) in V1 (Fig. 3A,B). Muscimol reduced V1 responses by 99 % ($P = 0.00001$, Wilcoxon signed rank test, 27 units, 6 animals, Fig. 3C). We did not check if the entirety of V1 was silenced, but the fluorescent muscimol had spread across V1 (Fig. 3B) and receptive fields of the silenced V1 neurons and the recorded sSC units were in the vicinity of each other for each experiment (Fig. 3D). Cortical silencing changed responses in the sSC in a manner depending on the unit and stimulus (Fig. 3E). On average, it reduced the sSC responses to the center and both surround stimuli (center: before muscimol: 9.2 ± 1.2 Hz, after muscimol: 7.1 ± 1.3 Hz, mean ± SEM, $P = 0.0004$, Wilcoxon signed rank test, 57 units, 9 mice; iso: 3.8 ± 0.6 Hz before muscimol, 2.9 ± 0.5 Hz after muscimol, $P = 0.018$, Wilcoxon signed rank test, 57 units, 9 mice; cross: before muscimol: 9.5 ± 1.2 Hz, after muscimol: 8.1 ± 1.2 Hz, $P = 0.03$, Wilcoxon signed rank test, 45 units, 8 mice, Fig. 3**F**). Relative to each other, the response to the center grating and to a center grating with an iso-oriented surround were equally affected by cortical silencing. The iso-oriented surround suppression was thus unchanged (SSI before muscimol: 0.62 ± 0.03, after muscimol: 0.62 ± 0.04, mean ± SEM, $P = 0.4$, Wilcoxon signed rank test, 57 units, 9 mice, Fig. 3G). This shows that surround suppression is not inherited from the visual cortex, and input from visual cortex possibly only changes the gain (Zhao et al. 2014). The response to a center grating with an iso-oriented surround were proportionally more reduced by cortical silencing than the responses to the cross-oriented surround (iso/cross response before muscimol: 0.42 ± 0.03, mean ± SEM; after muscimol: 0.35 ± 0.03; $P = 0.0025$, Wilcoxon signed rank test,

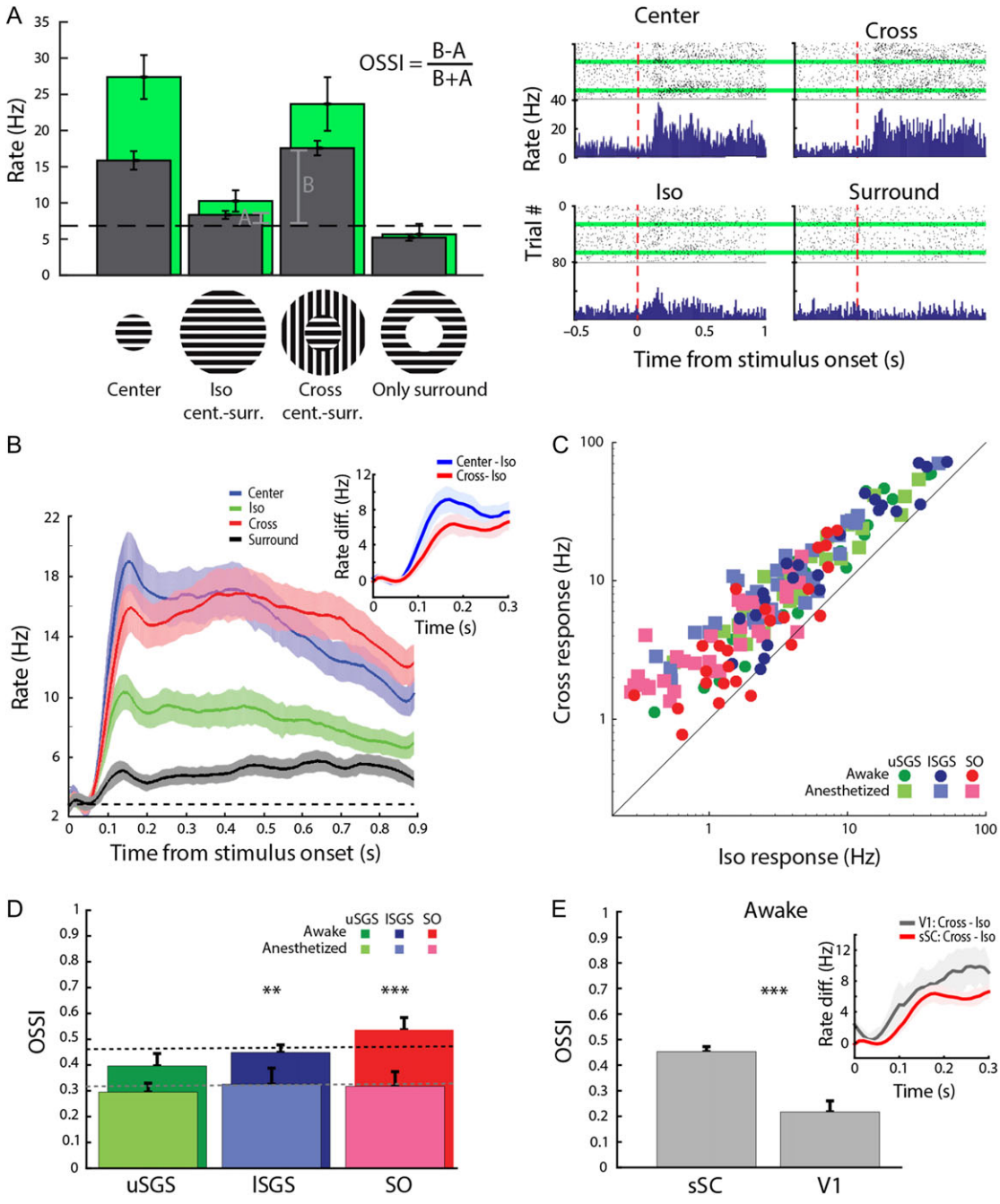

Figure 2. Orientation dependence of surround suppression in the sSC. (*A*) Left: Example responses to center only, center with an iso-oriented surround, center with a cross-oriented surround, and surround without center stimuli in awake sSC. Gray foreground bars show mean rates averaged over 16 directions. Green bars show mean rate for the 2 directions of the optimal orientation for the center only stimulus. Rates are mean firing rates during entire stimulus presentation. Dashed black line shows spontaneous firing. Error bars show SEM (5 repetitions per direction). Right: peri-stimulus spikes and spike histogram for the same neuron. Stimuli were shown randomized, but trials are here sorted by stimulus direction, which underlies the apparent rhythmic fluctuations in stimulus responses over trials. Highlighted in green are the 2 directions of the optimal orientation. (*B*) Population average peri-stimulus time spike histograms for the 4 conditions, averaged over all directions, in the awake mouse. Line and shading represent mean ± SEM. Dashed line shows the average spontaneous rate. The inset shows the time evolution of the difference between in rate between center and iso-condition and cross- and iso-condition. (*C*) Evoked responses for stimuli with a cross-oriented surround are larger than with an iso-oriented surround, in anesthetized (light coloured squares) and awake (saturated coloured disks) conditions. (*D*) Orientation-specific suppression index (OSSI) of sSC by layer, in anesthetized (light colours) and awake (saturated colours) conditions. Error bars show population median and bootstrapped error in median. Dashed lines represent median OSSI across layers for awake (black) and anesthetized (gray) conditions. Only laminar differences were in awake mice (**$P < 0.01$, ***$P < 0.001$ for comparisons with both other layers). (*E*) OSSI in the sSC and V1 of awake mice. Error bars show population median and bootstrapped error in the median. ***Denotes $P < 0.001$. The inset shows the development of the response difference between the iso- and cross-conditions in V1 and the sSC. Line and shading represent mean ± SEM.

Supplementary Fig. 6*A-B*). The absolute difference in response is not changed ($P = 0.29$, Supplementary Fig. 6 C), but the effect is that the orientation-specific suppression index increased upon cortical silencing (0.42 ± 0.03 before muscimol, 0.52 ± 0.05 after muscimol, mean ± SEM, $P = 0.003$, Wilcoxon signed rank test, 45 units, 8 mice, Fig. 3*H*). This does not depend on the 2 units with

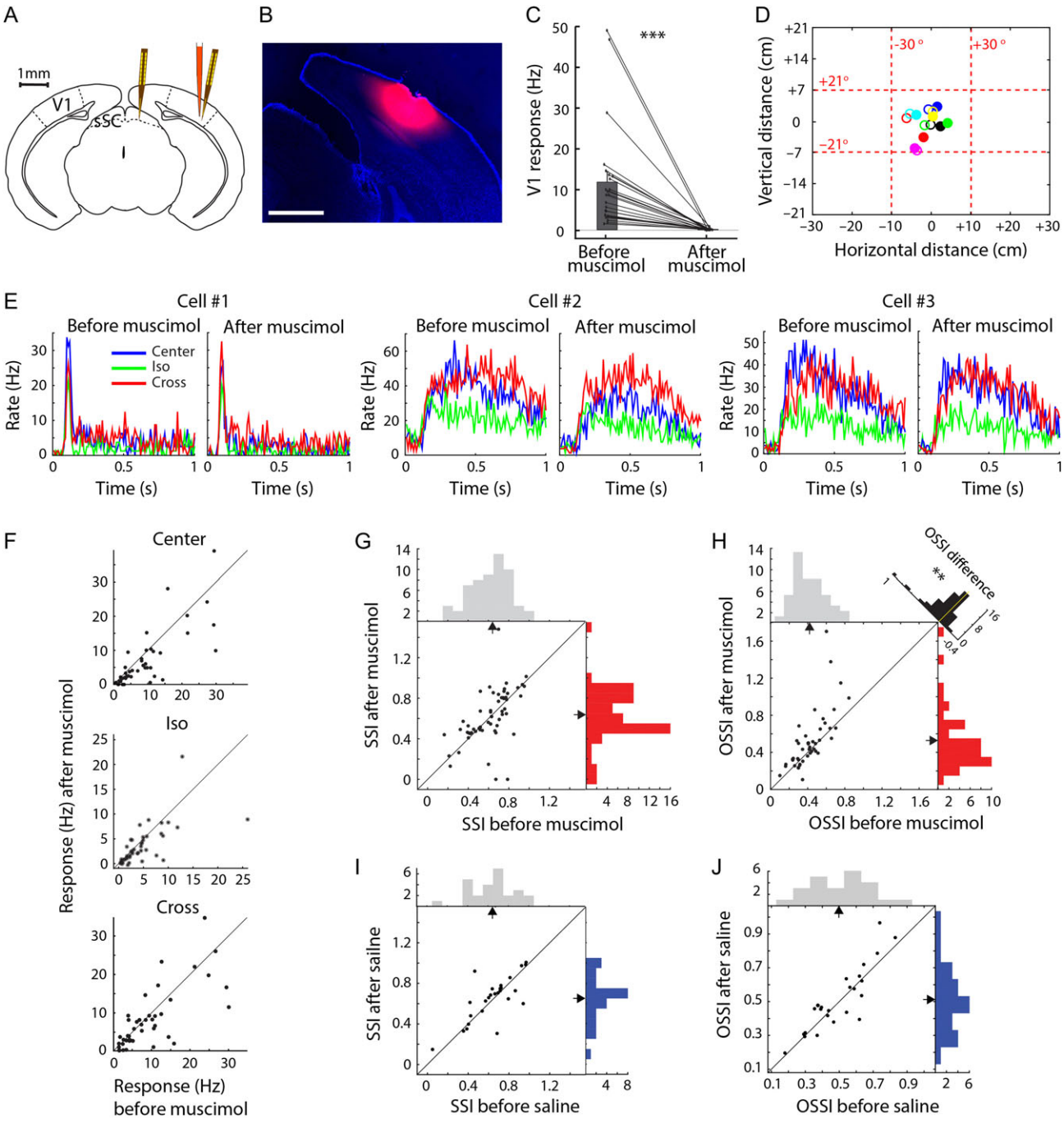

Figure 3. Silencing visual cortex does not affect iso-orientation suppression, but increases orientation-specific suppression index. (*A*) Schematic of a coronal brain section with probes in sSC and V1 and injection of fluorescent muscimol in V1 of awake mice. (*B*) Example spread of 100 nl of fluorescent muscimol in V1. Scale bar indicates 1 mm. (*C*) Responses in V1 before and after muscimol. Bars show mean. ***Indicate $P < 0.001$. (*D*) Dominant receptive field centers in V1 (nonfilled circles) and sSC (filled circles) for recordings from different mice. Different colors correspond to different mice. (*E*) Three examples of cell PSTHs in response to center (blue), iso (green), and cross (red) stimuli. (*F*) Responses to the center, iso and cross stimuli, from top to bottom respectively, in the sSC are reduced by cortical silencing. (*G*) Surround suppression index (for the iso-oriented surround) in the sSC is not affected by cortical silencing. (*H*) Orientation-specific suppression index in the sSC increases by cortical silencing. **Denotes $P < 0.01$. (without points with OSSI > 1.2, $P = 0.009$). (*I*) Surround suppression index in the sSC before and after saline injection in V1. (*J*) Orientation-specific suppression index in the sSC before and after saline injection in V1.

OSSI > 1.2 after muscimol injection (before muscimol: 0.42 ± 0.02, after muscimol: 0.48 ± 0.03, mean ± SEM, $P = 0.009$, Wilcoxon signed rank test, when these 2 units are removed). Responses to gratings with a cross-oriented surround were less reduced than the responses to the center grating alone (Supplementary Fig. 7). When we define a cross-orientation facilitation index (COFI), analogous to the iso-orientation surround suppression, as the difference in response to a center stimulus with and without a cross-oriented surround divided by the response to the center stimulus alone, we see that this is increased by cortical silencing (before: 0.17 ± 0.07, mean ± SEM; after 0.59 ± 0.12; $P = 8 \times 10^{-7}$, Wilcoxon signed rank test, Supplementary Fig. 7A).

Overall, we conclude that in the awake mouse, input from the visual cortex reduced the difference in response induced by orthogonally oriented surrounding gratings compared to parallel oriented surrounding gratings and enhanced the difference between center alone and with an orthogonal surround. For these stimuli, the influence of cortex is thus not only changing the gain, but also changing the response strengths relative to each other. The same recordings and manipulations using a saline control injection instead of muscimol did not reveal any significant differences before and after injection (response: $P = 0.75$; SSI: $P = 0.10$; OSSI: $P = 0.23$, 24 units, 4 mice, all Wilcoxon signed rank test, Fig. 3*I–J*).

Phenomenological Model

Although the effect of the corticotectal connections is to change the relative responses in the sSC, this does not automatically imply that there is very specific wiring between V1 and other cortical visual areas and the sSC. Indeed, our model shows that even retinotopically matched excitatory connections from V1 to all neurons in the sSC can account for the data. The model consists of a phenomenological description of a population of sSC neurons receiving retinotopically matched excitatory connections from the retina and V1 to the sSC, combined with surround inhibition in the sSC (see Materials and Methods section, Fig. 4A). The model does not include a description of the wiring within the sSC, except for an inhibition that is activated by surrounding stimuli. In the model, the non-cortical excitatory input to the sSC cells has an iso-oriented surround suppression profile that is similar to the measured surround suppression profile in visual cortex. The orientation specificity of the surround suppression of the non-cortical excitatory input, however, is higher than it is in visual cortex. Silencing visual cortex reduces the input for center and surrounds (Fig. 4B), but because it does not alter the ratio between center and iso-oriented surround, the mean SSI is not affected. The ratio between the input to parallel and orthogonal surrounds is changed by silencing cortex because it will more resemble the ratio of the combination of the retinal input and local excitatory connections, which is higher than the ratio in visual cortex. The model parameters were chosen such that the mean observables of the model match the experimental data within one standard error (Table 1). A random sample drawn from the model distribution gives an insignificant change in SSI ($P = 0.4$, Wilcoxon signed rank test, 45 units, Fig. 4C), while the change in OSSI is significant ($P = 0.01$, Wilcoxon signed rank test, 45 units, Fig. 4D), matching the measured data (Fig. 3*F–G*).

Discussion

We found strong surround suppression in the superficial layers of the mouse superior colliculus. Especially in the awake mouse, a grating evokes more response when it is surrounded by an orthogonally oriented grating than when it is surrounded by a parallel grating. The difference is larger than the response pop-out seen for these stimuli in the visual cortex. Silencing the visual cortex increased the difference between the responses to the grating with a parallel and orthogonal surround, showing that the existence of response pop-out in the sSC is not dependent on input from the visual cortex. On the contrary, collicular pop-out is reduced by cortical input.

Origin of Surround Suppression in the sSC

Previously, it was shown that neurons in the sSC of anesthetized animals show surround suppression (Sterling and Wickelgren 1969; Girman and Lund 2007; Gale and Murphy 2014), but we have shown that this is not homogenous across its depth in the anesthetized animal. We found that the SO layer of the sSC exhibits less surround suppression than the uSGS and has a larger optimal stimulus diameter. Retinal ganglion cells show center-surround organization in which a stimulus in the surround suppresses responses to the center stimulus (Barlow 1953), and in the mouse project to different sublamina of the sSC depending on their type (Hofbauer and Dräger 1985; Dhande and Huberman 2014). Retinal ganglion cell classes projecting to different layers show different optimal sizes, with cell types terminating in the contralateral top half of the sSC (W3, J and BD) on average preferring smaller sized stimuli than the W7 class terminating in the SO (Kim et al. 2010). Although a systematic review of the surround suppression of these cells is not available, the examples given in the study of Kim and colleagues suggest that the laminar differences in the amount of surround suppression in the retinal input to the sSC match that of the output. This poses the question how much surround suppression is inherited from the retina. Surround suppression in the optic tectum in zebrafish also matches its retinal input (Preuss et al. 2014), but this surround suppression, especially in the deeper layers, is not completely inherited from its retina (Del Bene et al. 2010). The orientation specificity that we found in the surround suppression also is suggestive of a post-retinal origin, as orientation selectivity is commonly seen as a property emerging further down the visual pathway. Some orientation selectivity, however, is already present in many mouse retinal ganglion cell responses (Zhao et al. 2013), and a surrounding grating drifting in the same

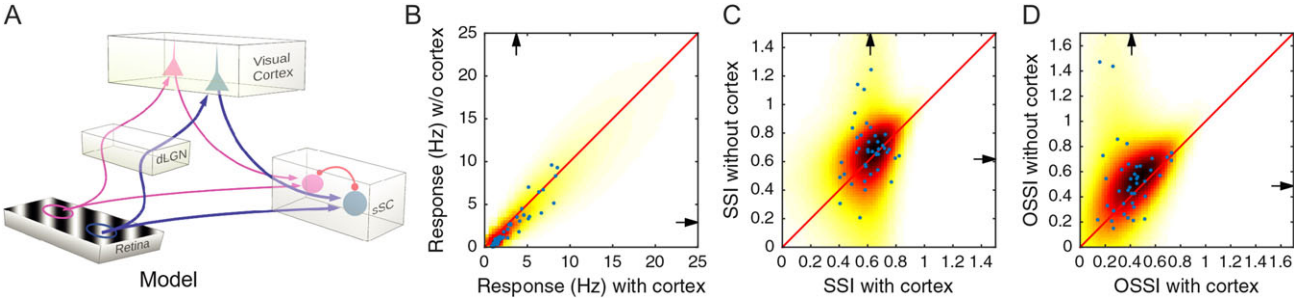

Figure 4. Simple model captures influence of visual cortex on sSC. (A) Input from visual cortex is retinotopically matched and excitatory. Orientation-unspecific lateral inhibition is operating in the sSC. (*B–D*) Density plots (gradients) of response, SSI and OSSI with and without visual cortex input into the model sSC. Arrowheads indicate the mean of the distributions. The dots are a randomly drawn sample of 45 cells, like the experimental data in Figure 3. For this sample, OSSI is shifted by silencing cortex ($P = 0.01$, Wilcoxon signed rank test), while SSI is not ($P = 0.4$).

direction as a center grating strongly reduces responses in some retinal ganglion cells in the vertebrate retina (Ölveczky et al. 2003). Furthermore, a study using stimuli similar to ours found qualitatively the same orientation dependence in the surround suppression of rat retinal ganglion cells as the modulation we found in the sSC (Girman and Lund 2010). It is thus likely that part of the surround modulation in the sSC is inherited from the retina. Another part of the surround modulation comes from local GABAergic activity in the superior colliculus (Kaneda and Isa 2013). Application of $GABA_A$ receptor antagonist bicuculline enhanced responses in the anesthetized rat sSC and increased the relative responses to large disks compared to that of smaller sizes (Binns and Salt 1997). Previously, surround suppression in awake mouse V1 was shown to depend partially on inhibition from local somatostatin-positive interneurons that have large optimal stimulus sizes (Adesnik et al. 2012). The categories of inhibitory neurons in the sSC are not well established, but in general GABAergic neurons in the sSC are horizontal cells with large optimal sizes (Gale and Murphy 2014). Iso-orientation surround suppression in V1 and sSC may thus have a common mechanism. However, 2-photon calcium imaging recently showed that size tuning in the full population of GABAergic neurons is identical to the size tuning of excitatory neurons (Kasai and Isa 2016). This suggests that long-range axons from inhibitory neurons are more likely to cause the surround suppression in the sSC than short-range axons from local interneurons with large optimal sizes, but this remains an open question.

Cortical Influence on the sSC

One possible alternative source of surround modulation of activity in the sSC is the visual cortex. The sSC receives input from layer 5 V1 pyramidal neurons. This corticotectal input is strong enough to directly induce behavior (Liang et al. 2015) and the response differences for the cross- and iso-oriented surrounds appear in the visual cortex not after they appear in the sSC. Apart from input from V1, the SC also receives input from the other visual areas (Wang and Burkhalter 2013). Size tuning in the sSC, however, was similar with and without visual cortex in anesthetized cat (Wickelgren and Sterling 1969). Also, in anesthetized rat the surround modulation in the uSGS was unaffected by ablation of the visual cortex (Girman and Lund 2007). The latter finding was interpreted as being due to the lack of direct cortical input into the uSGS, but recently it was shown that the influence of cortex is severely reduced by anesthesia. In anesthetized mice, silencing visual cortex made no difference in the collicular responses to looming disks, while in the awake animal sSC responses were strongly reduced when cortex was transiently silenced (Zhao et al. 2014). The speed tuning to stimuli was unaffected, suggesting that the visual cortex does not affect sSC feature selectivity but causes a gain enhancement. In contrast to only modulating the sSC gain, we found that cortex can change the responses to different stimuli relative to each other. Silencing visual cortex in the awake mouse reduced the responses in the sSC. The ratio of responses of a center grating and a grating with an iso-oriented surround was not changed. For gratings of one orientation, size tuning is thus not affected, but the relative responses to stimuli with a parallel or an orthogonal surround were influenced by the visual cortex. The effect of cortical input is to pull the OSSI towards its own level while leaving the SSI unchanged. It may seem a conundrum how the excitatory retinotopic connections from visual cortex can change the OSSI but not the SSI in the sSC. A simple phenomenological rate-based model was however enough to match the data. The main ingredients of the model are retinotopically matched excitatory corticotectal inputs, local inhibition in the sSC causing surround suppression and either local or retinal facilitation of cross-oriented surrounds. Of course, it is likely that there is more specificity in the corticotectal connections, which target both excitatory and inhibitory neurons but possibly not in equal proportion (Zingg et al. 2017), but this is not necessary to explain the data presented here.

Function of Surround Modulation in the sSC

The model explains the effect of visual cortical silencing on the orientation specificity of surround suppression, but it does not explain the mechanism or the reason behind the strong surround modulation in the superior colliculus and its specific orientation profile. Several functions have been suggested for surround suppression in the visual system. One suggestion is that suppression reduces the correlations in neuronal responses, leading to sparser coding (Barlow 1972; Vinje and Gallant 2000). A second is that it may mediate detection of orientation discontinuities or weak signals in noise (Levitt and Lund 1997). A third is that it may help to segregate objects in the foreground from the background (Roelfsema 2006). The fourth suggestion may be the most relevant to the superior colliculus. Attention will be drawn by local differences in orientation and movement (Joseph and Optican 1996), because they may indicate a behaviorally relevant object or animal in a visual scene. Surround suppression, and in particular the difference between iso-orientation and cross-orientation suppression, may represent a pop-out mechanism for detection (Knierim and van Essen 1992). The response pop-out seen in the primary visual cortex to cross-oriented stimuli is assumed to be the source of the increased saliency of these stimuli (Parkhurst and Niebur 2004; Boehler et al. 2009; Melloni et al. 2012; Zhang et al. 2012; Shushruth et al. 2013; Schmid and Victor 2014), but modulations in the superior colliculus could thus also underlie the perceptual pop-out, like in the homologous fish optic tectum (Ben-Tov et al. 2015). The mammalian superior colliculus is a key structure in directing an animal's attention (Knudsen 2007; Zénon and Krauzlis 2012), but it is thought to have lost its prerogative on form and object vision to the visual cortex, which may make a more high-level assessment of which stimuli are relevant. In the rodent, the superior colliculus is important in deciding whether to attend, capture, freeze or escape (Dean et al. 1989; Shang et al. 2015; Wei et al. 2015). It is unclear if freezing and escape in the primate can be directly initiated by visual input to the superior colliculus, but the superior colliculus is certainly important for target selection in the primate (McPeek and Keller 2004).

We might interpret our finding that silencing visual cortex in the awake animal increases the difference between an orthogonal and a parallel surround, as increasing the importance of low-level stimulus incongruencies in determining stimulus saliency. The perceptual pop-out of the odd-one-out may have a neural correlate in superior colliculus, which is not dependent on, but even in spite of cortical input.

Authors' Contributions

Conceptualization, Methodology, Software, Data Curation: M.A. and J.A.H.; Investigation, Validation, Formal Analysis, Writing—Review and Editing, Visualization: M.A.; Pupil tracking: A.T.; Resources, Writing—Original Draft, Supervision, Funding Acquisition: J.A.H.

Supplementary Material

Supplementary data are available at *Cerebral Cortex* online.

Funding

The Netherlands Organisation for Scientific Research (NWO VIDI 864.10.010).

Notes

We thank Simon Lansbergen for developing the pupil recording, Christiaan Levelt for his support and sharing mice and equipment, Pieter Roelfsema for sharing equipment, Ralph Hamelink, Hadi Saiepour, Matt Self and Joris Vangeneugden for advice. *Conflict of Interest*: None declared.

References

Adesnik H, Bruns W, Taniguchi H, Huang ZJ, Scanziani M. 2012. A neural circuit for spatial summation in visual cortex. Nature. 490:226–231.

Ahmadlou M, Heimel JA. 2015. Preference for concentric orientations in the mouse superior colliculus. Nat Commun. 6:6773.

Ayaz A, Saleem AB, Schölvinck ML, Carandini M. 2013. Locomotion controls spatial integration in mouse visual cortex. Curr Biol. 23:890–894.

Barlow HB. 1953. Summation and inhibition in the frog's retina. J Physiol. 119:69–88.

Barlow HB. 1972. Single units and sensation: a neuron doctrine for perceptual psychology? Perception. 1:371–394.

Ben-Tov M, Donchin O, Ben-Shahar O, Segev R. 2015. Pop-out in visual search of moving targets in the archer fish. Nat Commun. 6:6476.

Binns KE, Salt TE. 1997. Different roles for GABAA and GABAB receptors in visual processing in the rat superior colliculus. J Physiol. 504:629–639.

Blakemore C, Tobin EA. 1972. Lateral inhibition between orientation detectors in the cat's visual cortex. Exp Brain Res. 15: 439–440.

Boehler CN, Tsotsos JK, Schoenfeld MA, Heinze HJ, Hopf JM. 2009. The center-surround profile of the focus of attention arises from recurrent processing in visual cortex. Cereb Cortex. 19:982–991.

Cang J, Wang L, Stryker MP, Feldheim DA. 2008. Roles of ephrinas and structured activity in the development of functional maps in the superior colliculus. J Neurosci. 28:11015–11023.

Dean P, Redgrave P, Westby GW. 1989. Event or emergency? Two response systems in the mammalian superior colliculus. Trends Neurosci. 12:137–147.

Del Bene F, Wyart C, Robles E, Tran A, Looger L, Scott EK, Isacoff EY, Baier H. 2010. Filtering of visual information in the tectum by an identified neural circuit. Science. 330:669–673.

Dhande OS, Huberman AD. 2014. Retinal ganglion cell maps in the brain: implications for visual processing. Curr Opin Neurobiol. 24:133–142.

Feinberg EH, Meister M. 2015. Orientation columns in the mouse superior colliculus. Nature. 519:229–232.

Gale SD, Murphy GJ. 2014. Distinct representation and distribution of visual information by specific cell types in mouse superficial superior colliculus. J Neurosci. 34:13458–13471.

Girman S, Lund R. 2010. Orientation-specific modulation of rat retinal ganglion cell responses and its dependence on relative orientations of the center and surround gratings. J Neurophysiol. 104:2951–2962.

Girman SV, Lund RD. 2007. Most superficial sublamina of rat superior colliculus: neuronal response properties and correlates with perceptual figure-ground segregation. J Neurophysiol. 98: 161–177.

Girman SV, Sauvé Y, Lund RD. 1999. Receptive field properties of single neurons in rat primary visual cortex. J Neurophysiol. 82:301–311.

Heimel JA, Saiepour MH, Chakravarthy S, Hermans JM, Levelt CN. 2010. Contrast gain control and cortical TrkB signaling shape visual acuity. Nat Neurosci. 13:642–648.

Hofbauer A, Dräger UC. 1985. Depth segregation of retinal ganglion cells projecting to mouse superior colliculus. J Comp Neurol. 234:465–474.

Itti L, Koch C. 2001. Computational modelling of visual attention. Nat Rev Neurosci. 2:194–203. Review.

Joseph JS, Optican LM. 1996. Involuntary attentional shifts due to orientation differences. Percept Psychophys. 58:651–665.

Kaneda K, Isa T. 2013. GABAergic mechanisms for shaping transient visual responses in the mouse superior colliculus. Neuroscience. 235:129–140.

Kasai M, Isa T. 2016. Imaging population dynamics of surround suppression in the superior colliculus. Eur J Neurosci. doi:10.1111/ejn.13371.

Kim IJ, Zhang Y, Meister M, Sanes JR. 2010. Laminar restriction of retinal ganglion cell dendrites and axons: subtype-specific developmental patterns revealed with transgenic markers. J Neurosci. 30:1452–1462.

Kleiner M, Brainard D, Pelli D. 2007. What's new in Psychtoolbox-3? Perception. 36:1–16.

Knierim JJ, van Essen DC. 1992. Neuronal responses to static texture patterns in area V1 of the alert macaque monkey. J Neurophysiol. 67:961–980.

Knudsen EI. 2007. Fundamental components of attention. Annu Rev Neurosci. 30:57–78.

Levitt JB, Lund JS. 1997. Contrast dependence of contextual effects in primate visual cortex. Nature. 387:73–76.

Liang F, Xiong XR, Zingg B, Ji XY, Zhang LI, Tao HW. 2015. Sensory cortical control of a visually induced arrest behavior via corticotectal projections. Neuron. 86:755–767.

McPeek RM, Keller EL. 2004. Deficits in saccade target selection after inactivation of superior colliculus. Nat Neurosci. 7:757–763.

Melloni L, van Leeuwen S, Alink A, Müller NG. 2012. Interaction between bottom-up saliency and top-down control: how saliency maps are created in the human brain. Cereb Cortex. 22:2943–2952.

Ölveczky BP, Baccus SA, Meister M. 2003. Segregation of object and background motion in the retina. Nature. 423:401–408.

Parkhurst DJ, Niebur E. 2004. Texture contrast attracts overt visual attention in natural scenes. Eur J Neurosci. 19:783–789.

Pecka M, Han Y, Sader E, Mrsic-Flogel TD. 2014. Experience-dependent specialization of receptive field surround for selective coding of natural scenes. Neuron. 84:457–469.

Preuss SJ, Trivedi CA, vom Berg-Maurer CM, Ryu S, Bollmann JH. 2014. Classification of object size in retinotectal microcircuits. Curr Biol. 24:2376–2385.

Roelfsema PR. 2006. Cortical algorithms for perceptual grouping. Annu Rev Neurosci. 29:203–227.

Self MW, Lorteije JA, Vangeneugden J, van Beest EH, Grigore ME, Levelt CN, Heimel JA, Roelfsema PR. 2014. Orientation-tuned surround suppression in mouse visual cortex. J Neurosci. 34: 9290–9304.

Schmid AM, Victor JD. 2014. Possible functions of contextual modulations and receptive field nonlinearities: Pop-out and texture segmentation. Vision Res. 104:57–67.

Shang C, Liu Z, Chen Z, Shi Y, Wang Q, Liu S, Li D, Cao P. 2015. BRAIN CIRCUITS. A parvalbumin-positive excitatory visual pathway to trigger fear responses in mice. Science. 348:1472–1477.

Shushruth S, Nurminen L, Bijanzadeh M, Ichida JM, Vanni S, Angelucci A. 2013. Different orientation tuning of near- and far-surround suppression in macaque primary visual cortex mirrors their tuning in human perception. J Neurosci. 33:106–119.

Sterling P, Wickelgren BG. 1969. Visual receptive fields in the superior colliculus of the cat. J Neurophysiol. 32:1–15.

Vaiceliunaite A, Erisken S, Franzen F, Katzner S, Busse L. 2013. Spatial integration in mouse primary visual cortex. J Neurophysiol. 110:964–972.

Vanegas MI, Blangero A, Kelly SP. 2015. Electrophysiological indices of surround suppression in humans. J Neurophysiol. 113:1100–1109.

Vinje WE, Gallant JL. 2000. Sparse coding and decorrelation in primary visual cortex during natural vision. Science. 287: 1273–1276.

Wang Q, Burkhalter A. 2013. Stream-related preferences of inputs to the superior colliculus from areas of dorsal and ventral streams of mouse visual cortex. J Neurosci. 33: 1696–1705.

Wang L, Sarnaik R, Rangarajan K, Liu X, Cang J. 2010. Visual receptive field properties of neurons in the superficial superior colliculus of the mouse. J Neurosci. 30:16573–16584.

Wei P, Liu N, Zhang Z, Liu X, Tang Y, He X, Wu B, Zhou Z, Liu Y, Li J, et al. 2015. Processing of visually evoked innate fear by a non-canonical thalamic pathway. Nat Commun. 6:6756.

Wickelgren BG, Sterling P. 1969. Influence of visual cortex on receptive fields in the superior colliculus of the cat. J Neurophysiol. 32:16–23.

Zahar Y, Wagner H, Gutfreund Y. 2012. Responses of tectal neurons to contrasting stimuli: an electrophysiological study in the barn owl. PLoS One. 7(6):e39559.

Zénon A, Krauzlis RJ. 2012. Attention deficits without cortical neuronal deficits. Nature. 489:434–437.

Zhang X, Zhaoping L, Zhou T, Fang F. 2012. Neural activities in V1 create a bottom-up saliency map. Neuron. 73:183–192.

Zhao X, Chen H, Liu X, Cang J. 2013. Orientation-selective responses in the mouse lateral geniculate nucleus. J Neurosci. 33:12751–12763.

Zhao X, Liu M, Cang J. 2014. Visual cortex modulates the magnitude but not the selectivity of looming-evoked responses in the superior colliculus of awake mice. Neuron. 84:202–213.

Zingg B, Chou XL, Zhang ZG, Mesik L, Liang F, Tao HW, Zhang LI. 2017. AAV-mediated anterograde transsynaptic tagging: mapping corticocollicular input-defined neural pathways for defense behaviors. Neuron. 93:33–47.